

Structure and Properties of Dental Casting Gold Alloys
I. Determination of Ordered Structures in Solid Solutions of Gold,
Silver, and Copper by Interpretation of Variations
in the Unit Cell Length

MAUD BERGMAN,^a LARS HOLMLUND^a and NILS INGRİ^b

^a*Department of Dental Technology, University of Umeå, S-901 87 Umeå, and* ^b*Department of Inorganic Chemistry, University of Umeå, S-901 87 Umeå, Sweden*

Solid solutions of gold, silver, and copper equilibrated at 800°C were quenched to room temperature and values of the cubic unit cell length, a , were determined using X-ray powder diffraction. The total mol fractions were varied within the limits $X_{Au} = 0.33 - 0.83$, $X_{Ag} = 0 - 0.55$, $X_{Cu} = 0 - 0.67$, a composition range of interest in dentistry. In attempting to explain the experimentally determined cell lengths as a function of the composition, the existence of clusters was suggested. An equilibrium method for calculation of the compositions and amounts of clusters was proposed and the changes in the cell length were assumed to be linearly proportional to the mol fractions of the "species" present; the relation is given in eqn. (5). Experimental data were compared with those from different theoretical models and the model with the complexes A_3B , A_3C , AC , and AC_3 in addition to the free units A , B , C gave the best fit. In the formulae A , B , C stand for units with Au -, Ag -, and Cu -atoms, respectively. The formation constants for the complexes are presented in Table 2. A comparison with results from other types of measurements is given.

Casting gold alloys are used in dentistry for crown and bridge constructions, inlays and for details in removable partial prosthesis. Such dental applications require alloy materials of high strength and resistance against mastication forces and against corrosive attack by the fluids in the oral cavity. The gold alloys mostly used for these purposes are ternary (Au , Ag , Cu) alloys with additions of platinum, palladium, and zinc. By an appropriate heat treatment, at temperatures below 450°C, these alloys can be hardened and a tensile strength and a hardness unusually high for a nonferrous material can be obtained. However, this hardening heat treatment does not level out concentration gradients and conventional dental gold castings have been found to be far from homogeneous.^{1,2}

Inhomogeneity of dental gold alloys is said to be one of the factors contributing to the electrochemical process in oral corrosion.^{3,4} Metal migration from metallic dental restorative materials into hard and soft oral tissues has been demonstrated by Söremark *et al.*,^{5,6} Bergenholtz *et al.*⁷ and Angmar-Månsson *et al.*⁸ In comparison it may be of interest to note that traces of gold have been detected in the hair of persons who had been solely in external contact with gold (jewellery).⁹

It has been proposed that the metal migration implies a galvanic dissolution of colloidal or ionic particles (from the restorative materials) followed by a subsequent transportation of the particles to the various tissues, and that the dissolution is caused by potential differences between metallic materials of different composition surrounded by an electrolyte.

A number of symptoms attributed to galvanic corrosion in the oral cavity have been reported, *e.g.* metallic taste, increased salivation, mucous patches, erosions, leukoplakia, nerve shocks, burning tongue, indigestion, allergy, and nervous irritability.^{4,10-13} In addition discoloration of the metallic restoration is frequently found.

It is known from metallurgical techniques that with suitable heat treatment at high temperatures it is possible to level out concentration gradients within an alloy. This homogenization heat treatment is often called annealing. In dentistry the annealing (if actually carried out) is performed at 700–800°C and prior to the hardening heat treatment. During annealing the gold alloys undergo structural rearrangements, resulting in a change from a random arrangement to one in which part of the atoms are ordered, forming clusters (complexes). This cluster formation affects many of the physical properties of an alloy, *e.g.*, conductivity, hardness, tensile strength, and unit cell length. Exact knowledge of the cluster formation is therefore of great importance.

In the present communication we present an equilibrium method for calculation of compositions and amounts of clusters in solid solutions of a cubic gold alloy system using experimental X-ray powder data, *i.e.* unit cell lengths (a) as a function of the composition. The method has been applied to the system (Au, Ag, Cu) with special emphasis on compositions and temperatures of interest in dentistry.

MATERIALS AND METHODS

Metals used. Thirteen binary and twenty-four ternary alloys were prepared with the compositions given in Table 1. Round wires with a diameter of 0.5 mm were used. The purity was for gold and for silver min. 99.95 % (Nyström and Matthey, England). The copper was of the type SM-0010-02 with a purity of min. 99.90 % Cu containing 0.04 % oxygen (Svenska Metallverken, Sweden).

Specimen preparation. The pure metals were weighed out in proper proportions immediately after being treated for 1 min in 4 M H₂SO₄ (Ag, Cu) or 4 M HNO₃ (Au) to eliminate impurities and oxides on the surface. The wires were then immediately twisted together and melted in a crucible of recrystallised alumina (Degussit AL 23 containing >99.5 % Al₂O₃) in an electrically heated furnace with an inert atmosphere of argon (Aga, quality SR). The molten specimens were kept at 1100°C for 30 min, cooled in the furnace to 800°C, where they were kept for another 30 min, and then quenched by rapid cooling of the crucible in room tempered water.

Table 1. Experimental data a (X_{Au} , X_{Ag} , X_{Cu}) with standard deviation σ' . The table also presents the residuals Δ_1 and Δ_2 obtained from two model calculations. $\Delta_1 = (a_{exp} - a_{calc}) \times 10^3 \text{ \AA}$ (Vegard's law model) where a_{calc} has been calculated using $a_{Au} = 4.078$, $a_{Ag} = 4.086$, and $a_{Cu} = 3.615$; $\Delta_2 = (a_{exp} - a_{calc}) \times 10^3 \text{ \AA}$ where a_{calc} has been calculated using the complexes A_3B , A_3C , AC , AC_3 (final results of the present work). In addition the standard deviation, $\sigma'(a)$, obtained for the determination of the lattice parameter is given in $\text{\AA} \times 10^3$. The first part of the data given are those obtained from own determinations. The latter part of the data has been used only for calculations in the binary systems. The data within parentheses are data from the literature while the remainder has been obtained by extrapolation from our own determinations.

X_A , X_B , X_C , a , $\sigma'(a)$, Δ_1 , Δ_2 : 1, 0, 0, 4.078, 1, 0, 0; 0, 1, 0, 4.086, 1, 0, 0; 0, 0, 1, 3.615, 2, 0, 0; 0.83, 0.17, 0, 4.073, 1, -6, 2; 0.69, 0.31, 0, 4.072, 1, -8, 0; 0.62, 0.38, 0, 4.073, 1, -8, 0; 0.56, 0.44, 0, 4.074, 1, -8, -1; 0.55, 0.45, 0, 4.075, 1, -7, 0; 0.50, 0.50, 0, 4.075, 1, -7, -1; 0.45, 0.55, 0, 4.076, 1, -6, -2; 0.74, 0, 0.26, 3.981, 2, 23, 1; 0.65, 0, 0.35, 3.942, 2, 26, -2; 0.51, 0, 0.49, 3.879, 2, 28, -2; 0.48, 0, 0.52, 3.864, 1, 27, -3; 0.43, 0, 0.57, 3.844, 2, 30, 1; 0.33, 0, 0.67, 3.791, 2, 23, -1; 0.83, 0.09, 0.08, 4.048, 1, 6, 3; 0.70, 0.20, 0.10, 4.040, 2, 7, 1; 0.69, 0.17, 0.14, 4.025, 1, 10, 0; 0.64, 0.06, 0.30, 3.963, 1, 23, -1; 0.62, 0.14, 0.24, 3.988, 1, 20, 0; 0.61, 0.25, 0.14, 4.025, 1, 10, -1; 0.59, 0.34, 0.07, 4.054, 1, 6, 2; 0.55, 0.17, 0.28, 3.971, 1, 21, -1; 0.54, 0.17, 0.29, 3.969, 1, 24, 1; 0.54, 0.09, 0.37, 3.934, 1, 27, 0; 0.51, 0.27, 0.22, 3.994, 1, 16, -3; 0.50, 0.37, 0.13, 4.032, 1, 11, 1; 0.48, 0.45, 0.07, 4.054, 2, 5, 0; 0.48, 0.05, 0.47, 3.891, 2, 30, 1; 0.47, 0.12, 0.41, 3.919, 1, 30, 3; 0.45, 0.21, 0.34, 3.949, 2, 27, 3; 0.44, 0.29, 0.27, 3.975, 2, 20, -1; 0.42, 0.08, 0.50, 3.875, 1, 28, 0; 0.41, 0.38, 0.21, 4.000, 2, 16, 0; 0.39, 0.05, 0.56, 3.847, 2, 28, 1; 0.38, 0.23, 0.39, 3.924, 2, 25, 1; 0.38, 0.16, 0.46, 3.893, 1, 27, 1; 0.37, 0.04, 0.59, 3.831, 2, 26, 0; 0.35, 0.11, 0.54, 3.854, 1, 25, 0.

X_A , X_B , X_C , a : (0.10, 0.90, 0, 4.082; 0.20, 0.80, 0, 4.081; 0.30, 0.70, 0, 4.079; 0.40, 0.60, 0, 4.076; 0.80, 0.20, 0, 4.072; 0.90, 0.10, 0, 4.074;) 0.80, 0, 0.20, 4.003; 0.70, 0, 0.30, 3.965; 0.60, 0, 0.40, 3.921; 0.55, 0, 0.45, 3.898; 0.50, 0, 0.50, 3.875; 0.40, 0, 0.60, 3.828; 0.35, 0, 0.65, 3.804; 0.25, 0, 0.75, 3.755; 0.20, 0, 0.80, 3.728; 0.15, 0, 0.85, 3.700; 0.10, 0, 0.90, 3.672; 0.05, 0, 0.95, 3.643.

Powder specimens were prepared using an air-cooled dental coromant bur and care was taken to extract the powder from the inner parts of the specimen. During the powder preparation lattice distortions due to plastic deformation occurred. The lattice distortions caused a line broadening on the X-ray powder photograms. To reduce this effect the powder samples were put in small crucibles of Al_2O_3 for heat treatment at $800^\circ C$ in an argon atmosphere. In the annealing treatments samples of cold-worked powder were placed in a furnace which was pre-heated to $800^\circ C$. The time for heat treatment was selected to allow recrystallisation without any sintering of the powder particles. The crucibles with the powder specimens were quenched to room temperature.

The accuracy of the temperature measurements. The temperature control of the furnace, $\pm 10^\circ C$, was carried out with a Pt/Pt 10 % Rh thermocouple. The temperature was measured close to the crucible inside the furnace tube (60 cm by length and 5.5 cm i.d.) using other thermocouples of the same type. The thermopotentials were measured by a Leeds and Northrup Student's potentiometer (Cat. No. 7645) and read to ± 0.02 mV. A Norma galvanometer (measuring range 0.0018–20 μA) was used as a zero point instrument. Before every reading a standardization with a Weston Normal cell (1.01859 V, $20^\circ C$) was performed. The accuracy of the corresponding temperatures was $\pm 2^\circ C$.

The X-ray powder data. X-Ray powder diffraction photograms were taken of all the heat treated powders using a Guinier-Hägg camera and mainly the $CuK\alpha_1$ radiation ($\lambda = 1.54051$). All the structures observed were face centered cubic. For calibration of the camera constant, silicon ($a = 5.43054 \pm 0.00017 \text{ \AA}$ at $25^\circ C$)¹⁴ was used. The parameter $a \pm \sigma'(a)$ was calculated and refined using conventional methods.¹⁵ The values obtained are given in Table 1. Powder lines with differences between the calculated and observed

values of $\sin^2\theta$ greater than 0.0002 were omitted in the determination of the lattice parameters.

On the phase diagrams. The melting points for gold, silver, and copper are 1063, 960.5 and 1083°C, respectively. The gold-silver and gold-copper binary systems consist of continuous series of solid solutions. In the gold-silver system the melting temperature evenly falls from gold to silver. In the gold-copper system there is a minimum in the melting temperature at about 56 at. % gold (889°C) and at lower temperatures ordered phases, especially AuCu and AuCu₃ are found. Beside these two phases, Au₂Cu₃ and Au₃Cu have been considered as formulas on which superlattices may be based. The silver-copper system is eutectic with the eutectic point at 39.9 at. % copper and 779°C.¹⁶ The ternary system of gold-silver-copper is characterized by a solid solubility gap and a two-phase region in which copper-poor and silver-poor phases coexist. Isothermal sections defining the two-phase region of the ternary phase diagram have been constructed using data from McMullin and Norton¹⁷ (Fig. 1).

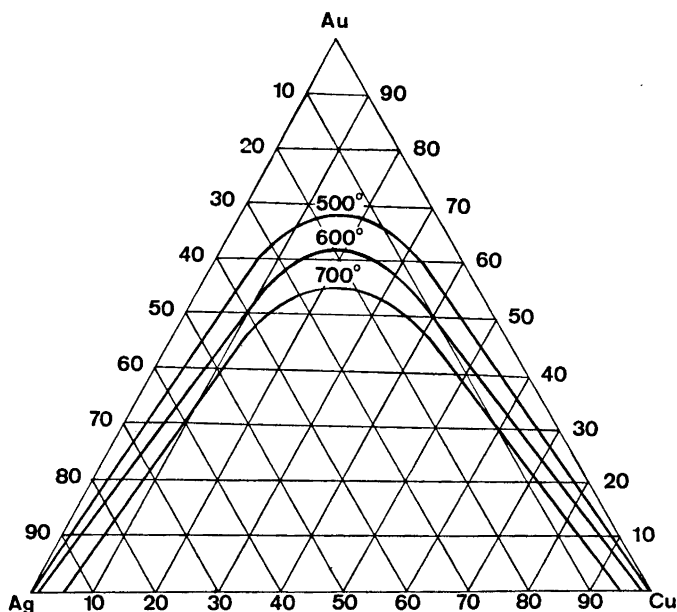


Fig. 1. Isothermal sections defining the two phase region in the (Au, Ag, Cu) system (The diagram was constructed after McMullin and Norton, 1949, using wt. % and °C.)

In the gold-corner (more than 60 wt. % gold) of the ternary diagram there is a single phase region with solid solutions between $\approx 650^\circ\text{C}$ and the melting temperatures of the alloys in question. In odontological work only the ternary gold alloys with a gold content of 75 wt. % or more are of interest. However, in the complex alloys with the metals of the platinum group the gold content may be lower.

CALCULATIONS AND RESULTS

Our experimental data a as a function of the composition X_A , X_B , X_C are collected in Table 1 for all compositions investigated. Together with these data literature data have also been used in the Au-Ag system.¹⁸ Extrapolated values have been used in the binary Au-Cu system.

Models considered. We begin the calculations by testing a model without taking cluster formation into consideration. The alloy crystals are assumed to be built up of equally sized and randomly ordered "unit cells" A, B, and C. Hereafter we shall use the concept "unit" instead of "unit cell". The units A contain only gold atoms, B only silver atoms and C only copper atoms. Furthermore, the unit cell length, a , is assumed to be linearly dependent on the mol fractions of A, B, and C (extension of Vegard's law). This dependency may be written:

$$a = a_A x_A + a_B x_B + a_C x_C \quad (1)$$

where x_A , x_B , and x_C are the fractions of units A, B, and C, respectively. In this particular case, $x_A = X_A$, $x_B = X_B$, and $x_C = X_C$, where X_A , X_B , and X_C are the total mol fractions of gold, silver, and copper atoms, respectively. The constants a_A , a_B , and a_C are the unit cell lengths for $x_A = 1$, $x_B = 1$, and $x_C = 1$ (cell dimensions of the pure metals). For these constants we have used: $a_A = 4.078 \pm 0.001 \text{ \AA}$, $a_B = 4.086 \pm 0.001 \text{ \AA}$, and $a_C = 3.615 \pm 0.002 \text{ \AA}$, which were obtained from our own determinations. These values are in good agreement with the corresponding values given in the literature.¹⁹

An attempt to fit this simple Vegard's law model to our experimental data, $a(X_A, X_B, X_C)$, gives the result shown in Fig. 2. The figure presents the

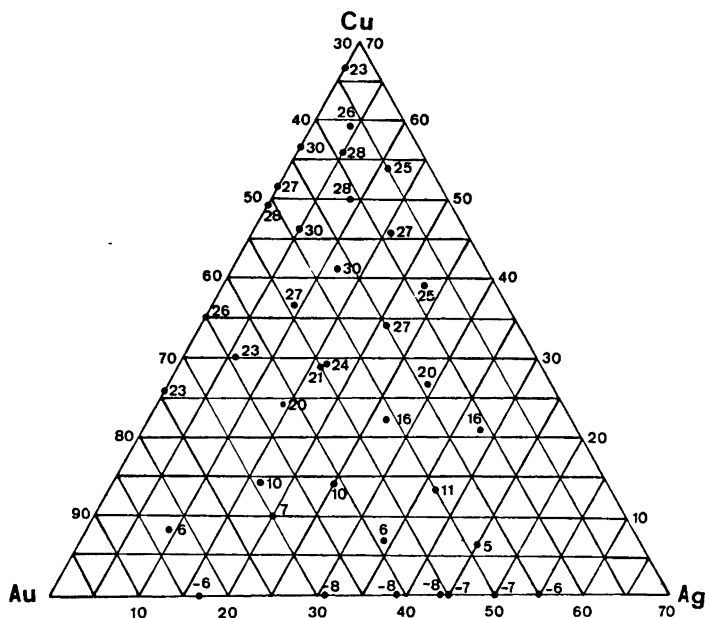


Fig. 2. The residuals $(a_{\text{exp}} - a_{\text{calc}}) \times 10^8 \text{ \AA}$ as a function of the composition X_{Au} , X_{Ag} , X_{Cu} . The quantity a_{calc} has been calculated assuming the validity of an extended Vegard's law relation; see eqn. (1). The diagram illustrates the effects which have to be explained.

residuals ($a_{\text{exp}} - a_{\text{calc}}$) for the best fit as a function of the fractions X_A , X_B , X_C . There are marked residuals in the region from $X_A = 0.75$, $X_C = 0.25$ through $X_A = 0.40$, $X_B = 0.30$, $X_C = 0.30$ to $X_A = 0.35$, $X_C = 0.65$. The magnitude of these residuals is for many compositions as much as 25–30 mÅ. These differences are too large to be ascribed to experimental errors alone and may therefore indicate the existence of some kind of interaction (*e.g.* the formation of clusters).

In order to test the hypothesis of cluster formation, we have constructed a theoretical model in which, in addition to the free units A, B, and C, more complex units (complexes) $A_p B_q C_r$ are permitted, p , q , and r being integers. Furthermore we will assume that the units $A_p B_q C_r$ are in equilibrium with the free units A, B, and C. Thus $pA + qB + rC \rightleftharpoons A_p B_q C_r$.

The law of mass action and the conditions for the total mol fractions X_A , X_B , and X_C then give:

$$X_A = x_A + p \beta_{pqr} x_A^p x_B^q x_C^r \quad (2)$$

$$X_B = x_B + q \beta_{pqr} x_A^p x_B^q x_C^r \quad (3)$$

$$X_C = x_C + r \beta_{pqr} x_A^p x_B^q x_C^r \quad (4)$$

Then, in analogy with (1), the expression for the unit cell length, a , will be:

$$a = a_A x_A + a_B x_B + a_C x_C + \sum_0^i a_{A_p B_q C_r} x_{A_p B_q C_r} \quad (5)$$

where i is the number of complexes, and $x_{A_p B_q C_r}$ the fraction of units $A_p B_q C_r$, and $a_{A_p B_q C_r}$ the unit cell length in a pure $A_p B_q C_r$ crystal.

In order to obtain the numbers and compositions of complexes present as well as the values of the parameters β_{pqr} and a_{pqr} , we have used a trial and error method based on the least squares principle. In this method, different models (sets of pqr values) are systematically tested on our experimental data a_{exp} , X_A , X_B , and X_C , and that model giving the lowest error square sum

$$U = \sum (a_{\text{exp}} - a_{\text{calc}})^2$$

is considered to be the best one. The calculations have been performed using the SPEFO version of the computer program LETAGROPVRID. For the principles of this computation method, see Refs. 20, 21, and 22. Note that in the calculations with the cluster models the use of X_A , X_B and X_C implies an approximation and was necessary due to the construction of the computer program.

Results of the model calculations. The calculations were begun by first analyzing each of the two binary systems Au–Ag and Au–Cu. The results are presented in Table 2. Here we can see that in the system Au–Ag, it is possible to explain the data with a single complex, either A_2B , A_3B , or A_4B_2 , of which A_2B gives the lowest error squares sum. However, the differences in error squares sum between the three possibilities are small and the mean error in a , $\sigma(a)$, for each of the complexes is within the accuracy of the measurements. It is possible then that complex combinations giving mean compositions in the neighbourhood of A_2B , A_3B , and A_4B_2 might also give possible explanations for our binary Au–Ag data.

Table 2. The results of the present study in terms of the complexes tested and the corresponding best constants. The equilibrium constant β_{pqr} is defined by the expressions (2), (3), and (4), and the constant a_{pqr} by eqn. (5).

Number of points tested	pqr tested	Error square sum $\times 10^{-5}$	$\sigma(a) \times 10^3$	$\beta_{pqr} \pm \sigma(\beta_{pqr})$		$a_{pqr} \pm \sigma(a_{pqr})$	
15	4 1 0	7.6	2.5	1.4	± 0.7	20.16	± 0.03
15	3 1 0	3.6	1.7	1.1	± 0.5	16.14	± 0.01
15	2 1 0	1.1	1.0	1.2	± 0.6	12.133	± 0.004
15	8 2 0	16	3.6	3.6	± 2.0	39.7	± 0.2
15	6 2 0	8.0	2.5	2.7	± 1.4	31.87	± 0.09
15	4 2 0	3.1	1.6	2.1	± 1.0	24.05	± 0.03
20	3 0 1	198	11	1.5	± 0.7	16.46	± 0.07
20	3 0 2	78	6.7	2.0	± 0.8	20.50	± 0.07
20	3 0 1	16	3.3				
	1 0 3						
20	5 0 4	84	7.5				
	4 0 5						
20	3 0 2	3.4	1.4	0.230	± 0.001	32	± 1
	2 0 3			89	± 67	19.26	± 0.01
20	3 0 1	1.8	1.1	632	± 114	15.93	± 0.01
	1 0 1			0.935	± 0.004	8.46	± 0.05
	1 0 3			33	± 32	14.99	± 0.01
40	3 0 2	13	2	66180	± 1008	19.65	± 0.01
	2 0 3			192	± 49	19.25	± 0.02
	2 1 0			0.12	± 0.10	11.77	± 0.05
40	3 0 1	8.1	1.5	639	± 1	15.92	± 0.01
	1 0 1			0.90	± 0.02	8.68	± 0.06
	1 0 3			3.9	± 2.8	14.66	± 0.08
	3 1 0			0.342	± 0.003	15.96	± 0.03

With the binary Au – Cu data, we found that among models with only one complex it was difficult to fit a suitable model to the data ($\sigma(a)$ too large). The search was thus extended to models with two and three coexisting complexes. We then found that a model with the complexes A_3C , AC , and AC_3 gave a good fit, being much better than that with A_3C and AC_3 alone.

In the next step in our analysis we extended the calculations to include the three-dimensional data in addition to the binary data. We then found that this range could be explained with binary complexes alone and that these complexes were A_3B , A_3C , AC , and AC_3 . Attempts to introduce ternary complexes or binary Ag – Cu complexes did not lead to a more probable explanation.

It should be mentioned that in those models in which the errors were calculated on the basis of cell volume instead of the cell edge, rather large error squares sums were obtained and it was thus difficult to fit the data with suitable complexes.

Complex distributions. Our results given as distributions of clusters and components as a function of X_{Ag} and X_{Cu} for three values of X_{Au} are shown in Fig. 3.

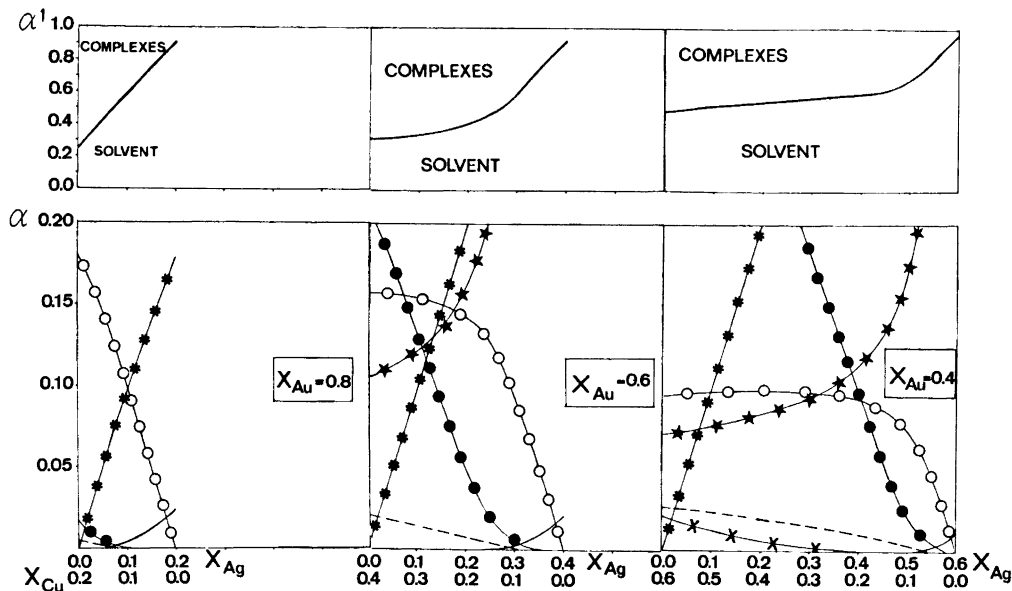


Fig. 3. The distribution of clusters and components as a function of X_{Ag} and X_{Cu} for three different values of X_{Au} : 0.80, 0.60 and 0.40.

- *—*— represent fractions of units A.
- » » » » B.
- » » » » C.
- » » » » A_3C .
- — — » » » » AC.
- x—x— » » » » AC_3 .
- — — » » » » A_3B .

$$\alpha^1 = \frac{x_A + x_B + x_C}{X_A + X_B + X_C}$$

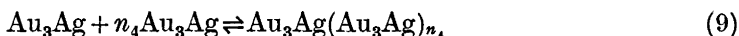
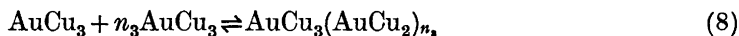
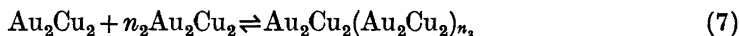
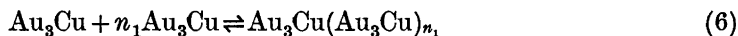
$$\alpha = \frac{x_{A_3B} + x_{AC_3}}{X_A + X_B + X_C}$$

It is seen from the diagrams that the complex A_3C is a rather strong complex and exists over nearly the whole concentration range studied. The maximum amounts are found at compositions around $X_A = 0.75$, $X_C = 0.25$, $X_B = 0$. The molar ratio of the complexes AC, AC_3 , and A_3B never exceeds the value 0.03 and represents minor complexes over the range studied. It is interesting to note that the A_3C complex is such a strong complex that especially in the gold-rich alloys the concentrations of free C are so low that the solvent may be regarded as a pure (A-, B)-solvent. At compositions of interest in dentistry, A_3C and AC are the only complexes which need to be considered and the distribution between complexes and components are about equal (see Fig. 3).

CONCLUSIONS AND PLAUSIBLE STRUCTURAL INTERPRETATIONS

In the solid (Au, Ag, Cu) solutions studied, the variations in the cell edge, a , with the composition have been interpreted as resulting from formation of the clusters (complexes) A_3B , A_3C , AC , AC_3 . These complexes may be imagined as being randomly suspended in a matrix of disordered A, B, and C units and the compositions and the amounts of the clusters being determined by the law of mass action. Furthermore, each of the species present is assumed to affect the cell length as described by eqn. (5). To explain the data with solely independent components A, B, and C was found impossible.

We have expressed the complexes in terms of units A, B, and C. As seen from expressions (2), (3), and (4) the sizes of the units can be arbitrarily chosen and depending on this choice the chemical formula of the complex may differ. If we assume four atoms in each of the units, the complex A_3C becomes $Au_{12}Cu_4$ and the complex AC becomes Au_4Cu_4 and so on. This means that the equilibrium calculations cannot give the correct sizes of the complexes. They provide the smallest multiple for each of the complexes and thus the notation A_3C refers to a single complex $(Au_3Cu)_N$ where N is an unknown integer. In addition we found that sets with two or more $(A_3C)_N$ -complexes could explain our data as well as a single A_3C -complex. The same behaviour was also found for the minor complexes. We may sum up by saying that it is impossible, with the data of the present work, to obtain a clear decision whether single complexes or series of complexes are present. However, the computer calculations clearly give the mean composition of the complexes. In this situation we may tentatively propose that the alloys are built up of series of complexes, formed according to a core and link mechanism.²³ For the different complex series the mechanism may be written:



where n may attain consecutive values from 1 up to infinity. All n -values need not be present. A restricted number of n -values is perhaps more probable. For determinations of formation constants in cases with such a mechanism a number of simplifications can be used. The most common approach is to simplify it to a two parameter problem. Such a set of parameters would of course also be possible to determine from the present data. However, we found such a calculation quite unnecessary, since the complexes are quantitatively well characterized by a "single complex" constant (used in the calculations of the distribution diagrams). On the basis of the proposed mechanism we will now try to give our result a plausible structural interpretation.

Each of the atoms Au, Ag, and Cu behaves in the matrix as if it were independent (complete disorder). Each is surrounded by twelve nearest and six near neighbours. In the most gold-rich alloys this environment consists of Au-atoms only. Furthermore the Cu- and Ag-atoms are here well separated from each other by Au-atoms. The forces between the atoms are mainly deter-

mined by the Au-atoms, and hence it follows that interactions Cu–Au and Ag–Au can be put equal to Au–Au. However, when the gold content decreases atoms Cu–Cu and Ag–Ag come closer and closer together. At the same time the probability increases that the Au-atoms in the near Au-sphere around the Cu- and Ag-atoms will be replaced by Cu- and Ag-atoms. When this occurs attractive forces appear and atoms Cu–Cu and Ag–Ag are coupled together. A coupling is achieved first when atoms Cu–Cu and Ag–Ag approach to within distances of a Å or $a/\sqrt{2}$ Å from each other. This corresponds to replacements of “near” and “nearest” Au-atoms, respectively. Through the “near” replacements the complexes $\text{CuAu}_3(\text{CuAu}_3)_n$ and $\text{AgAu}_3(\text{AgAu}_3)_n$ are formed and through the “nearest” replacements the complex $\text{CuAu}(\text{CuAu})_n$ results. As the Cu-content increases further “nearest” Au-replacements occur resulting in formation of the complexes $\text{AuCu}_3(\text{AuCu}_3)_n$, and finally one obtains isolated Au-atoms completely surrounded by a great number of Ag- and Cu-atoms.

COMPARISON WITH OTHER MEASUREMENTS

Lattice parameters. In previous reports it has been found that the parameters of the face centered cubic lattice in the (Au, Cu) system show a weak positive deviation from additivity.^{24,25} These results are also confirmed by the data of the present study. The lattice parameter *versus* composition curve in the (Au, Ag) system shows a minimum in the region of 70 at. % gold according to Sachs and Weerts²⁶ and Wiest¹⁸ and in the region of 50 at. % gold according to Nygaard and Vegard.²⁷ In agreement with these studies the present investigation has shown that an addition of silver to gold results in a contraction of the gold lattice. The minimum value of the lattice parameter was found at 69 at. % gold.

Determination of lattice parameters of alloys in the ternary (Au, Ag, Cu) system has been carried out by Masing and Kloiber²⁸ and Raub.²⁹ However, these investigations were performed under conditions (other temperatures and concentration ranges) which differ somewhat from those of the present study and thus direct comparisons are not possible. However, a similar trend in the values can be found.

Activity measurements. Ölander³⁰ measured the potential of the cell Ag/AgCl, KCl(l)/(Ag,Au) between 400°C and 625°C for seventeen compositions of the alloy electrode. $\log f_{\text{Ag}}(X_{\text{Ag}})$ at 530°C was given diagrammatically and we have replotted these results in Fig. 4. Due to the great difference between the temperature at which Ölander's measurements were performed and the temperature from which our alloys were quenched, a direct comparison is difficult. However, we have attempted to adjust our equilibrium constant for A_3B to determine whether our data could be made to fit those of Ölander. Even with a very high value of the constant (500 000) the fit cannot be considered as good. However, Ölander points out that only alloys with $X_{\text{Ag}} > 0.6$ gave stable potentials and hence no accurate measurements could be made with alloys richer in gold. Wagner and Engelhardt³¹ also measured the Ag-activity using emf-measurements and the same cell as Ölander. The tem-

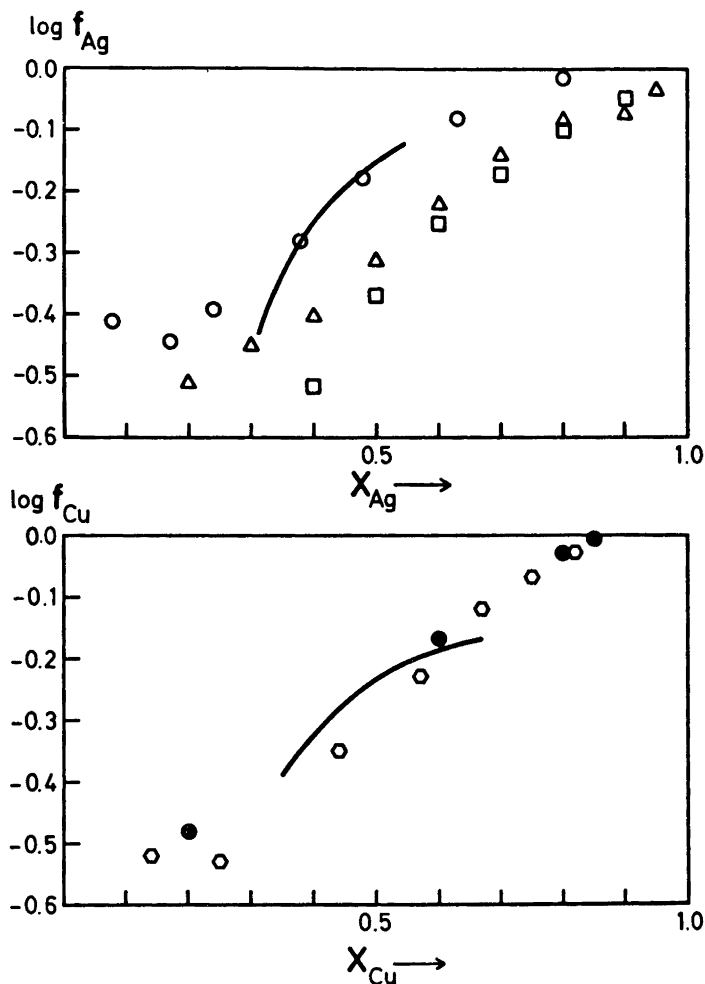


Fig. 4. A comparison of some previously obtained activity data with the results of the present study. The full curve given has been obtained through recalculation of our data to $\log f$ data.

$$\left(f_{Ag} = \frac{x_{Ag}}{X_{Ag}}, f_{Cu} = \frac{x_{Cu}}{X_{Cu}} \right)$$

The constants used for obtaining the full curve are given in the text. The symbols represent data from the literature. Δ Ölander, 1931, 530°C; \circ Wagner and Engelhardt, 1932, 745°C; \diamond Wagner and Engelhardt, 1932, 604°C; \square Wachter, 1932, 200°C; \bullet Trondsen and Bolsaitis, 1970, 825°C.

perature range was 410–745°C. In Fig. 4 we have plotted their values of $\log f_{Ag}(X_{Ag})$. Using the model which assumes the presence of the complex A_3B and a value for the equilibrium constant of 1600, it was possible to explain their data at 745°C in the region $X_{Ag} = 0.35 - 0.55$. The fit is shown in Fig. 4.

Wagner and Engelhardt³¹ also point out that at $X_{\text{Ag}} < 0.4$ the value of f obtained from their measurements was higher than expected from extrapolation of the measurements at higher Ag-concentrations. Wachter³² measured the Ag activity using the cell Ag(s)/AgCl(s)/Ag,Au (s.sol.) between 200 and 400°C, a temperature range which makes comparisons with our data difficult.

Wagner and Engelhardt³¹ also measured the potential of the cell Cu/CuCl, KCl(l)/(Cu,Au) for different compositions of the alloy electrode at 390, 527, and 604°C. Their data of $\log f_{\text{Cu}}(\bar{X}_{\text{Cu}})$ have been plotted in Fig. 4. Our results have been plotted in the same diagram after multiplying the values of our equilibrium constants for A_3C , AC, and AC_3 by a factor of 2.0. As can be seen, at $X_{\text{Cu}} < 0.6$ our curve is situated slightly above the values of Wagner and Engelhardt. In the region $X_{\text{Cu}} = 0.35 - 0.55$ good agreement was obtained between our model and the results obtained from activity measurements by Trondsen and Bolsaitis.³³ However, at $X_{\text{Cu}} > 0.55$ results deviating from those of the present study are found. Trondsen and Bolsaitis³³ used an emf-cell of the type Pt/Cu - Au(alloy) + $\text{Cu}_2\text{O}/0.85 \text{ ZrO}_2 - 0.15 \text{ CaO}/\text{Cu} + \text{Cu}_2\text{O}/\text{Pt}$ and obtained activity data for seven different alloy compositions in the temperature range 721 - 916°C. The fit is shown in Fig. 4.

It would be of particular interest to use a cell and directly measure activities in the ternary system also and then test the measurements with the model proposed in the present work.

Electrical conductivity. The electrical conductivity (κ) at 20°C for the pure Au, Ag, and Cu metals is 43×10^4 , 63×10^4 , $58 \times 10^4 \text{ ohm}^{-1} \text{ cm}^{-1}$, respectively. In the (Au, Ag) system there is a minimum in electrical conductivity at about 50 at. % ($\kappa \approx 9 \times 10^4 \text{ ohm}^{-1} \text{ cm}^{-1}$). The deviations after different pretreatments of the alloys are in most cases less than 1 %.³⁴ Alloys in the (Au, Cu) system quenched from high temperatures have values of the electrical conductivity which, in relation to the composition, lie on a continuous broadly U-shaped curve with a very flat minimum in the region of 55 at. % gold ($\kappa = 5.9 \times 10^4 \text{ ohm}^{-1} \text{ cm}^{-1}$). For the same alloys, slowly cooled after annealing at about 370°C, the curve of conductivity *versus* composition is still U-shaped but there are marked maxima at 25 and 50 at. % gold ($\kappa = 17.7 \times 10^4$ and $17.8 \times 10^4 \text{ ohm}^{-1} \text{ cm}^{-1}$).³⁵

In the ternary (Au, Ag, Cu) system, near the compositions AuCu - Ag and AuCu₃ - Ag, the values of the specific electrical conductivity for quenched alloys are about 8×10^4 and $10 \times 10^4 \text{ ohm}^{-1} \text{ cm}^{-1}$. Already when these alloys contain 5 at. % silver the conductivity values are not greatly affected by annealing.³⁶ However, only a restricted number of such measurements are available from the literature. When these results are fitted into our model we may conclude that the complexes AC_3 and AC seem to affect the conductivity to a great extent, whereas the contributions from the complexes A_3C and A_3B appear negligible. Moreover, one may note that relatively small silver amounts seem to reduce the influence of the complexes AC_3 and AC. For odontological purposes an alloy of low conductivity is preferable.

Thermal conductivity. Hirabayashi³⁷ investigated the specific heat capacity-temperature relation for a gold-copper alloy containing 74 at. % gold which had been annealed at 200°C for 20 days and slowly cooled to room temperature. A distinct peak on the curve was observed at 243°C. Moreover the specimen

after annealing at 200°C for 1 month showed several superstructure lines in the microphotometer trace of its X-ray back reflection photograph. Quenched alloys of the same composition had a less pronounced maximum value of the specific heat capacity-temperature curve at 229°C. This investigation would indicate the existence of an ordered structure A_3C (Au_3Cu).

Hardness measurements. Both (Au, Cu) and (Au, Ag) alloys quenched from high temperatures have a hardness maximum at 50–55 at. % gold ($H_B \approx 120$ and 25, respectively). Slowly cooled or annealed (Au, Cu) alloys have minimum values of the hardness in the 25 and 50 at. % gold region ($H_B \approx 45$ and 127) and maximum values corresponding to 45 and 55 at. % gold ($H_B \approx 190$). The hardness of the (Au, Ag) alloys is somewhat increased after quenching from lower temperatures.³⁴

We have carried out some preliminary Vickers hardness tests on all the alloys investigated in the present study, both binary and ternary. The distribution of the hardness values is in good agreement with results from previous studies.³⁸ We found that the hardness rises from the Au–Ag edge when the Cu-content increases. The maximum values are obtained at or near the Au–Cu edge at a composition around 50 at. %.

By using the equilibrium constants obtained from our best model we have obtained the amounts of species at different compositions. The distribution of the clusters and components has then been compared with the hardness values. The maximum hardness seem to be obtained when the component ratio $x_{Cu}/x_{Au} \approx 3$. Further work on hardness measurements is in progress.

Electron diffraction studies. Thin films of Au_3Cu were prepared by the evaporation method. Imperfect but sufficient, order was found in the specimens after annealing at about 200°C for 100–200 h. The films, whose transmission photographs showed clear superlattice rings, were then heated step by step up to 400 or 500°C and examined by electron diffraction after being quenched from several temperatures in the course of the heating. The estimated extent of the ordered zone decreased with temperature rise (19 Å at 250°C and 16 Å at 300°C). At high temperatures above the critical point on the specific heat capacity-temperature curve, photographs still showed faint broad bands of (110), which indicated that small ordered zones existed (14 Å at 400°C and 11 Å at 500°C).³⁹ These results coincide well with those obtained by Germer *et al.*⁴⁰ who found ordered zones in the $AuCu_3$ alloy. The size of these zones in $AuCu_3$ was 38 Å at 247°C, 21 Å at 349°C, and 11 Å at 560°C. However, according to Germer, the ordered alloy of $AuCu$ gave no sign of diffuse bands at temperatures above 400°C.

X-Ray diffuse scattering studies. Greenholz and Kidron⁴¹ state that at 500°C about one-third of the volume of an alloy with the composition Cu–Au is in the form of ordered zones, and that the mean size of the ordered zones is about $(3 \times 3 \times 3)$ unit cells. (In the present work we have found that for alloys of the composition Cu–Au, quenched from 800°C, about 60 % of the cell volume is occupied by clusters.) Greenholz and Kidron⁴¹ have obtained their results by calculations using both a statistical method and a method with a model of ordered zones embedded in a disordered matrix. (Data taken from Roberts⁴² were used.) Similar calculations on alloys with the composition Cu_3Au have shown that at 450°C 77 % of the cell volume was occupied by

the ordered zones and that about 60 % of the ordered volume is made up of zones with a size of $(1 \times 1 \times 1)$ unit cells, and about 34 % of it is in zones with a size of $(3 \times 3 \times 3)$ unit cells. They found no zones with a volume of $(2 \times 2 \times 2)$ unit cells. Gehlen and Cohen⁴³ have performed computer simulation work to find the substructure of disordered alloys. In the case of Cu_3Au held at 450°C they found ordered zones in a disordered matrix, and the zones were around 12 Å. (Data from Moss⁴⁴ and Raether⁴⁵ were used.)

The proposed models of ordered nuclei in an otherwise disordered matrix is a model which seems to have support also in kinetic studies.⁴⁶ The result of the present work fits very well into this picture. However, it would be of interest to make X-ray diffuse scattering studies for other alloy compositions, for instance in the range of Au_3Cu and for ternary compositions.

Acknowledgements. Our grateful thanks are due to docent Erik Rosén for fruitful discussions and to Fil. lic. Lage Pettersson for valuable help with the computer calculations. We also wish to thank Dr. Michael Sharp who revised the English manuscript. Financial support was given by the *Swedish Medical Research Council*, grant K70-24X-3043-01.

REFERENCES

1. Björn, E. and Hedegård, B. *Acta Odontol. Scand.* **23** (1965) 323.
2. Söremark, R., Freedman, G., Goldin, J. and Gettleman, L. *J. Dental. Res.* **45** (1966) 1723.
3. Spreng, M. *Schweiz. Monatsschr. Zahnheilk.* **50** (1940) 158.
4. Hedegård, B. *Trans. Roy. Sch. Dent.*, Stockholm and Umeå. **1** (1958) 3.
5. Söremark, R., Ingels, O., Plett, H. W. and Samsahl, K. *Acta Odontol. Scand.* **20** (1962) 215.
6. Söremark, R., Wing, K., Olsson, K. and Goldin, J. *J. Prosthetic Dentistry* **20** (1968) 531.
7. Bergenholtz, A., Hedegård, B. and Söremark, R. *Acta Odontol. Scand.* **23** (1965) 135.
8. Angmar-Månsson, B., Önnell, K.-Å. and Rud, J. *Odontol. Revy* **20** (1969) 245.
9. Söremark, R. *Personal communication* (1971).
10. Lain, E. S. *J. Am. Med. Ass.* **100** (1933) 717.
11. Keresztesi, K. *Z. Stom. (Wien)* **48** (1951) 429.
12. Reinwald, U. *Zahnärztl. Welt* **8** (1953) 31.
13. Frykholm, K. O., Friothiof, L., Fernström, Å. I. B., Moberger, G., Blohm, S. G. and Björn, E. *Acta Determato-Venerol.* **49** (1969) 268.
14. Parrish, W. *Acta Cryst.* **13** (1960) 838.
15. Hägg, G. *Fasanalys och identifiering med röntgendiffraktionsmetoder*, Compendium 1954, University, Uppsala, Sweden.
16. Hansen, M. *Constitution of Binary Alloys*. McGraw, New York, Toronto, London 1958.
17. McMullin, J. G. and Norton, J. T. *J. Metals* **1** (1949) 46.
18. Wiest, P. *Z. Physik* **81** (1933) 121.
19. *Crystal Data, Determinative Tables*, 2nd Ed., Washington 1963.
20. Ingri, N. and Sillén, L. G. *Arkiv Kemi* **23** (1964) 97.
21. Sillén, L. G. and Warnqvist, B. *Arkiv Kemi* **31** (1969) 377.
22. Pettersson, L., Andersson, I., Lyhamn, L. and Ingri, N. *Trans. Roy. Inst. Technol., Stockholm 1972. In press.* An article in *Contributions to Coordination Chemistry in Memory of L. G. Sillén*. Allmänna Förlaget, Stockholm 1972.
23. Sillén, L. G. *Acta Chem. Scand.* **8** (1954) 299, 318.
24. van Arkel, A. E. and Basart, J. *Z. Krist.* **68** (1928) 475.
25. Vegard, L. and Kloster, A. *Z. Krist.* **89** (1934) 560.
26. Sachs, G. and Weerts, J. *Z. Physik* **60** (1930) 481.
27. Nygaard, O. and Vegard, L. *Skrifter Norske Videnskaps-Akad. Oslo, I. Mat. Naturv. Kl.* **2** (1947) 37.

28. Masing, G. and Kloiber, K. *Z. Metallk.* **32** (1940) 125.
29. Raub, E. *Z. Metallk.* **40** (1949) 46.
30. Ölander, A. *J. Am. Chem. Soc.* **53** (1931) 3577.
31. Wagner, C. and Engelhardt, G. *Z. Physik. Chem. (Leipzig)* **A 159** (1932) 241.
32. Wachter, A. *J. Am. Chem. Soc.* **54** (1932) 4609.
33. Trondsen, J. and Bolsaitis, P. *Met. Trans.* **1** (1970) 2022.
34. *Gmelins Handbuch der anorganischen Chemie*, 8. Aufl., Systemnummer 60 (1955), 61 (1970), 62 (1954).
35. Kurnakow, N., Zemczuzny, S. and Zasedatelev, M. *J. Inst. Metals* **15** (1916) 305.
36. Bumm, H. *Z. Metallk.* **31** (1939) 318.
37. Hirabayashi, M. *J. Phys. Soc. Japan* **6** (1951) 129.
38. Leuser, J. *Metall* **3** (1949) 105.
39. Ogawa, S. and Watanabe, D. *J. Appl. Phys. Japan* **22** (1951) 1502.
40. Germer, L. H., Haworth, F. E. and Lander, J. J. *Phys. Rev.* **61** (1942) 614.
41. Greenholz, M. and Kidron, A. *Acta Cryst.* **A 26** (1970) 306, 311.
42. Roberts, B. W. *Acta Met.* **2** (1964) 598.
43. Gehlen, P. C. and Cohen, J. B. *Phys. Rev.* **139** (1965) 844.
44. Moss, S. C. *J. Appl. Phys.* **35** (1964) 3547.
45. Ræther, H. *Z. Angew. Phys.* **4** (1952) 53.
46. Krivoglaz, M. A. and Smirnow, A. A. *The Theory of Order-Disorder in Alloys*, Macdonald, London 1964, p. 55.

Received November 19, 1971.

KEMISK BIBLIOTEK
Den kgl. Veterinær- og Landbohøjskole